Electronic Supplementary Information

White-Light-Emitting Lanthanide and Lanthanide-Iridium Doped Supramolecular Gels: Modular Luminescence and Stimuli-Responsive Behaviour

Tufan Singha Mahapatra,*[a] Harwinder Singh,[a] Arunava Maity,[a] Ananta Dey,[a] Sumit Kumar Pramanik,[a] Eringathodi Suresh[a] and Amitava Das*[a]

[a]Analytical and Environmental Science Division and Centralized Instrument Facility, CSIR-Central Salt & Marine Chemicals Research Institute, Bhavnagar 364002, Gujarat, India. E-mail: tufansmp@gmail.com, a.das@csmcri.res.in

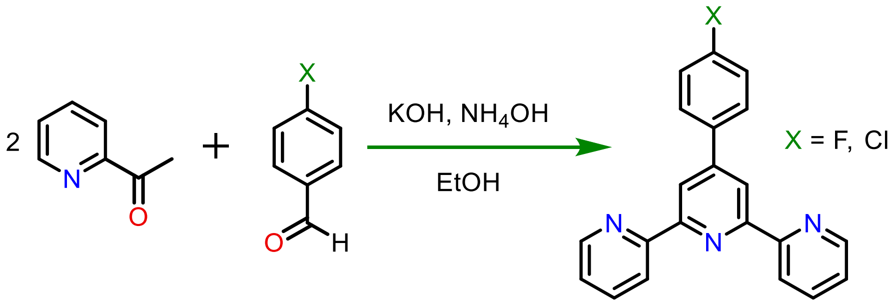

Scheme S1. Facile one-pot synthesis of 4′-p-halophenyl-2,2′:6′,2″-terpyridine

Characterization of L-F and L-Cl

L-F

Yield: (3.588 g, 45.67%). ^{1}H NMR (500 MHz, $CDCl_3$) δ 8.71 (d, *J* = 4.6 Hz, 2H), 8.67 (s, 2H), 8.65 (d, *J* = 8.0 Hz, 2H), 7.90–7.83 (m, 4H), 7.33 (dd, *J* = 7.0, 5.0 Hz, 2H), 7.22–7.13 (m, 2H). HRMS (ESI): calcd for $C_{21}H_{15}N_3F$ $[M+H]^+$ 328.1250 found 328.1289 and calcd for $C_{21}H_{14}N_3FNa$ $[M+Na]^+$ 350.1069 found 350.1091.

L-Cl

Yield: (3.490 g, 42.30%). ^{1}H NMR (500 MHz, $CDCl_3$) δ 8.71 (d, *J* = 4.4 Hz, 2H), 8.68 (s, 2H), 8.64 (d, *J* = 7.9 Hz, 2H), 7.88–7.79 (m, 4H), 7.46 (d, *J* = 8.6 Hz, 2H), 7.36–7.30 (m, 2H). HRMS (ESI): calcd for $C_{21}H_{15}N_3Cl$ $[M+H]^+$ 344.0955 found 344.0967.

Table S1. Crystal Parameters and Refinement Data for **L-F**.

Compound reference	**L-F**
Chemical formula	$C_{21}H_{14}N_3F$
Formula Mass	327.35
Crystal system	Monoclinic
Space group	$P2_1/c$
Crystal color	Colourless
Crystal size/mm^3	0.49×0.08×0.06
a/Å	3.8357(9)
b/Å	21.751(5)
c/Å	18.396(5)
α/°	90.0
β/°	92.713(4)
γ/°	90.0
V/Å^3	1533.0(6)
Z	4
D_c/g cm^{-3}	1.418
μ (mm^{-1})	0.094
F(000)	680
T/°K	150(2)
Total reflns	7902
R(int)	0.0433
Unique reflns	3001
Observed reflns (I > 2σ(I))	2519
Parameters	282
R_1 (I > 2σ(I)) wR$_2$(all reflns)	0.0775,0.1546
GOF (F^2)	1.200
CCDC number	1837781

$R_1 = \Sigma(\,||F_o|-|F_c||\,)/\Sigma|F_o|$. $wR_2 = [\,\Sigma w(|F_o|-|F_c|)^2/\Sigma w(F_o)^2]^{1/2}$. $w = 0.75/(\sigma^2(F_o) + 0.0010F_o^2)$

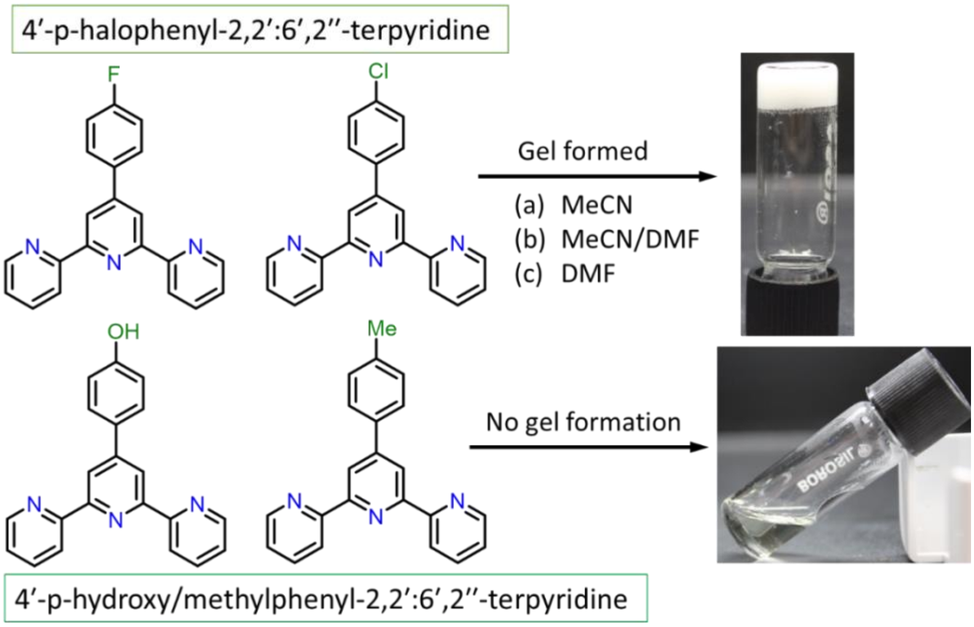

Scheme S2. Role of halogen atom in terpyridine moiety in gel formation

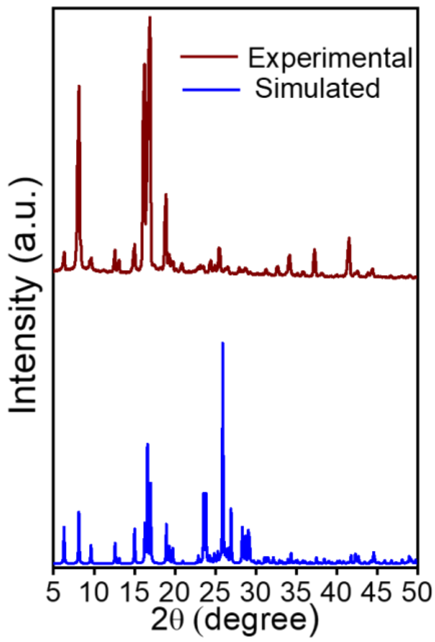

Fig. S1. Comparison of experimental (blue line) and simulated (brown line) PXRD patterns for L-F

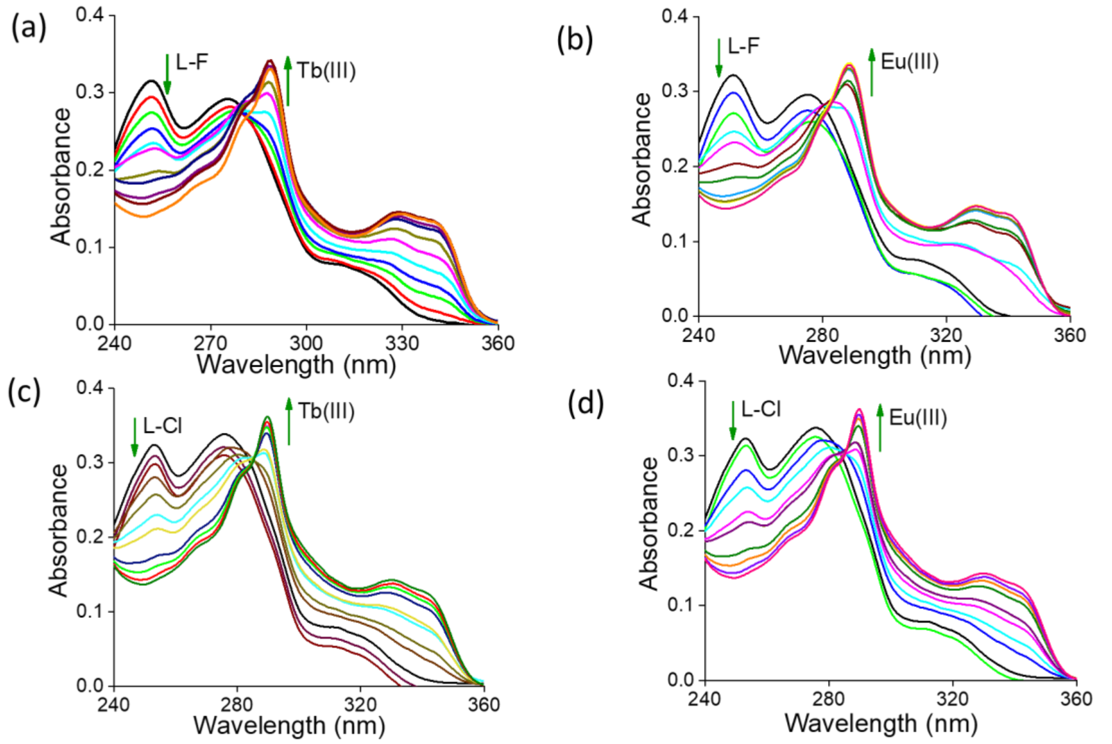

Fig. S2. Changes in the absorption spectra of (a and b) L-F (1×10^{-5} M) after addition of Tb(III) and Eu(III) (0 → 1 equiv) and (c and d) L-Cl (1×10^{-5} M) after addition of Tb(III) and Eu(III) (0 → 1 equiv) in MeCN.

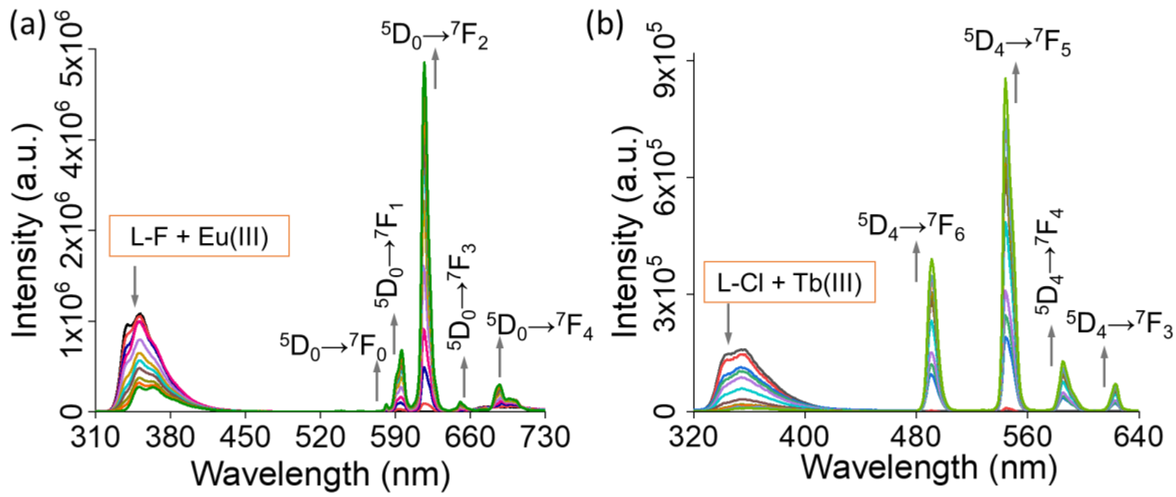

Fig. S3. Spectral changes in (a) the Eu(III) and (b) Tb(III) centred luminescence spectra upon titrating L-F or L-Cl (1.0×10^{-5} M) with Tb(III)/Eu(III) (0 → 1 mole equiv) in MeCN.

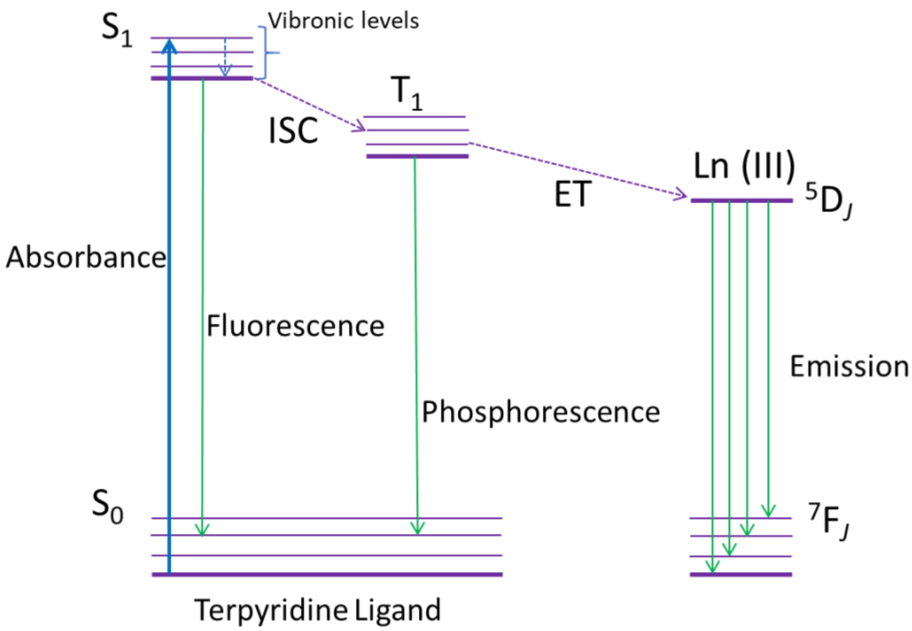

Scheme S3. Characteristic energy level diagram describing a general mechanism for emissive chromophore-appended lanthanide complexes sensitized through a ligand-centred triplet excited state (ISC- intersystem crossing, ET- Energy Transfer).

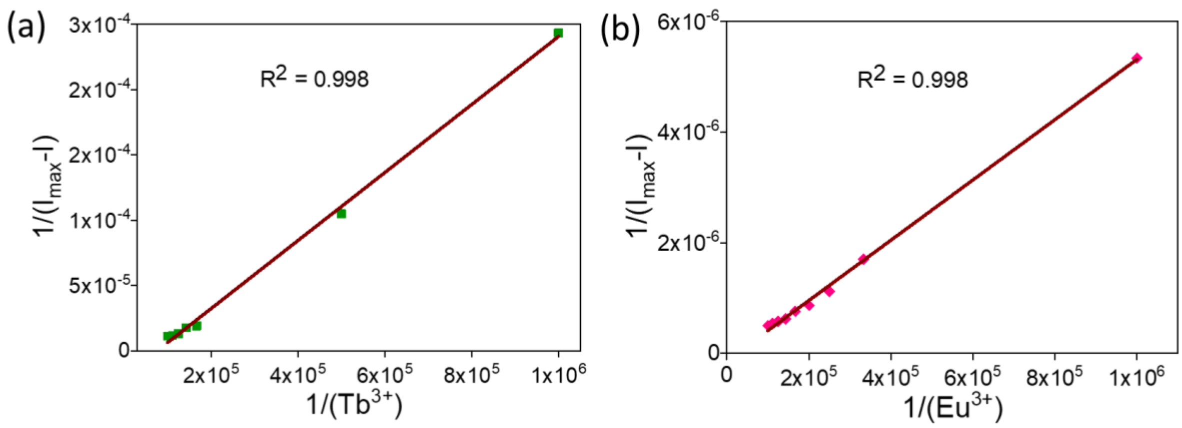

Fig. S4. Benesi-Hildebrand (B-H) plots obtained from the emission titration of (a) L-F (1 x 10^{-5} M) with Tb(III) and (b) L-Cl (1 x 10^{-5} M) with Eu(III) supported 1:1 binding stoichiometry (R^2 = 0.998).

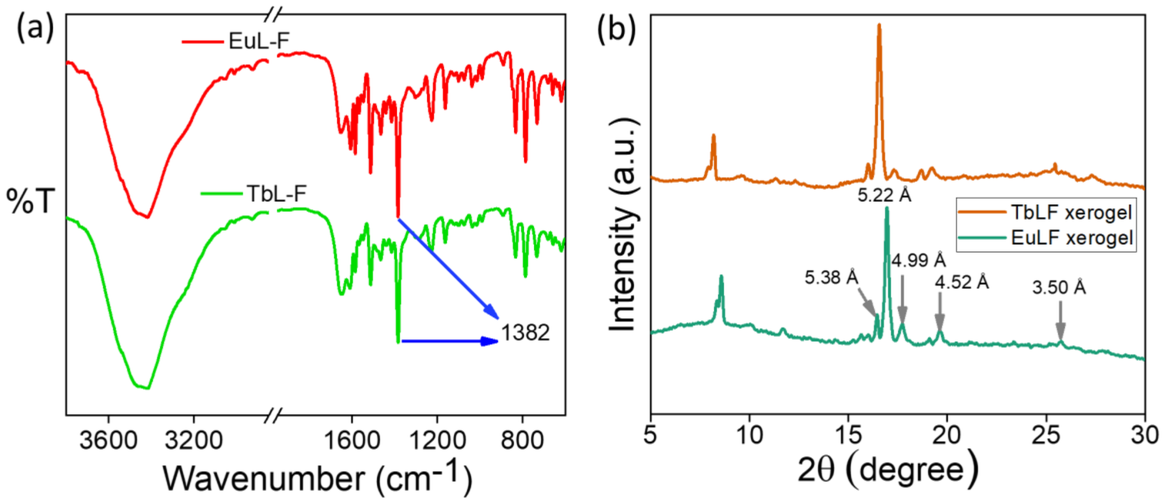

Fig. S5. (a) Comparison of (a) FT-IR spectra of Eu•L-F and Tb•L-F xerogels and (b) PXRD patterns of Eu•L-F and Tb•L-F xerogels.

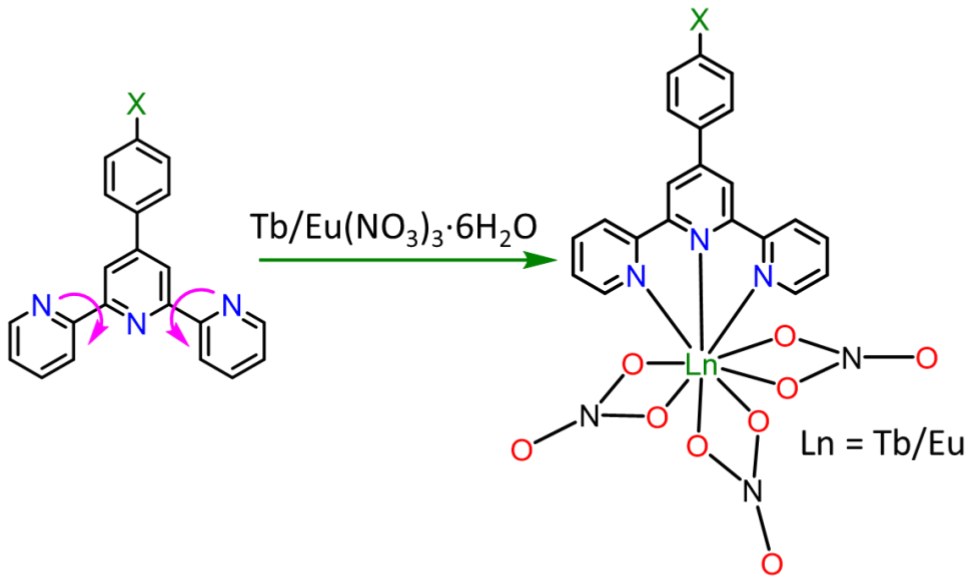

Scheme S4. Probable coordination environment around Eu(III) and Tb(III) in Eu•L-X and Tb•L-X (X = F and Cl)

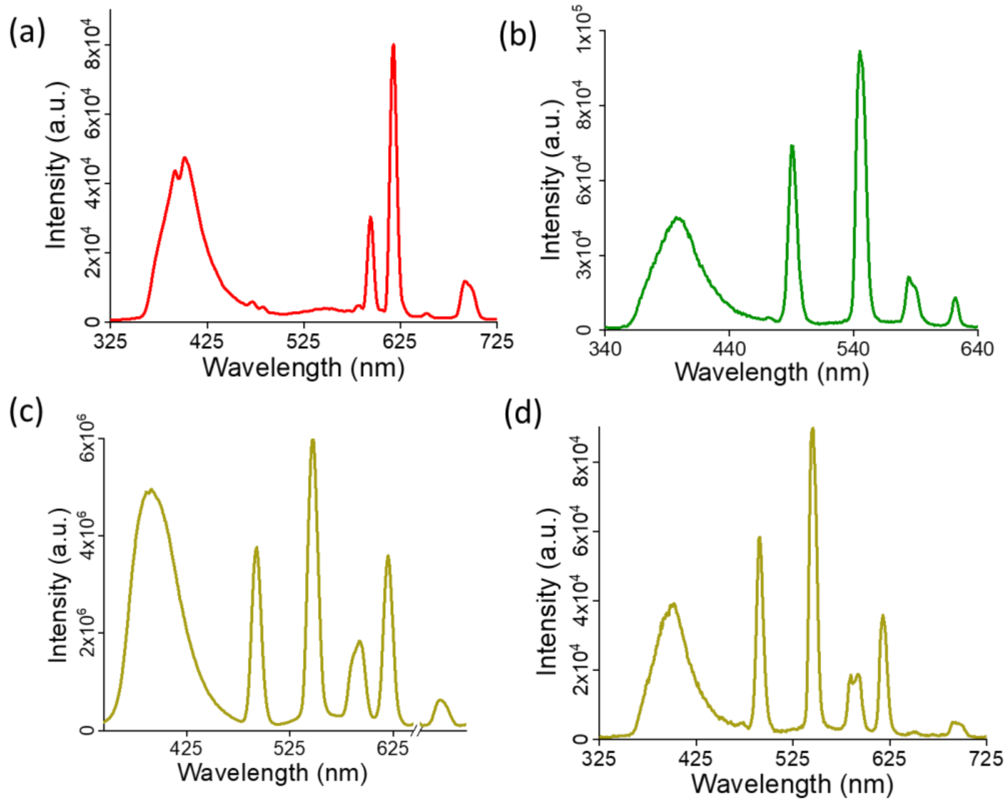

Fig. S6. Luminescence spectra of (a) Eu•L-Cl, (b) Tb•L-Cl, (c) Eu•L-Cl-Tb•L-Cl, and (d) Eu•L-Cl-2(Tb•L-Cl).

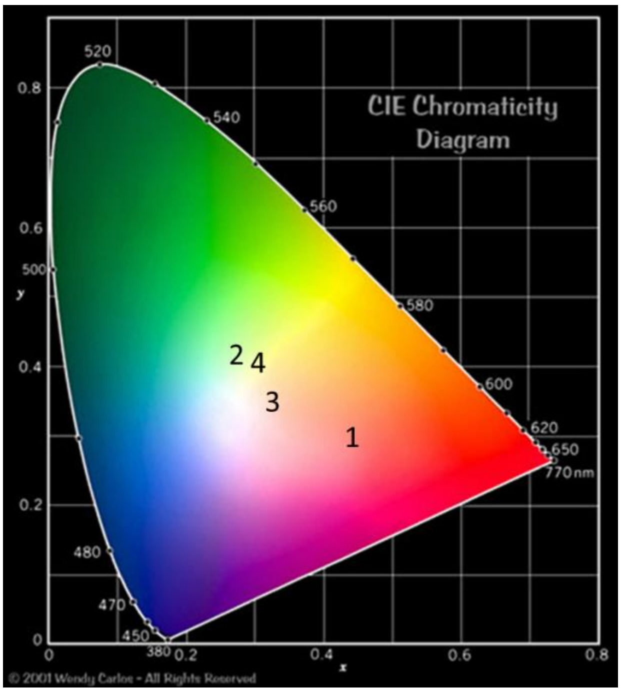

Fig. S7. CIE chromaticity diagram of Eu•L-Cl (1), Tb•L-Cl (2), Eu•L-Cl-Tb•L-Cl (3), and Eu•L-Cl-2(Tb•L-Cl) (4) gels

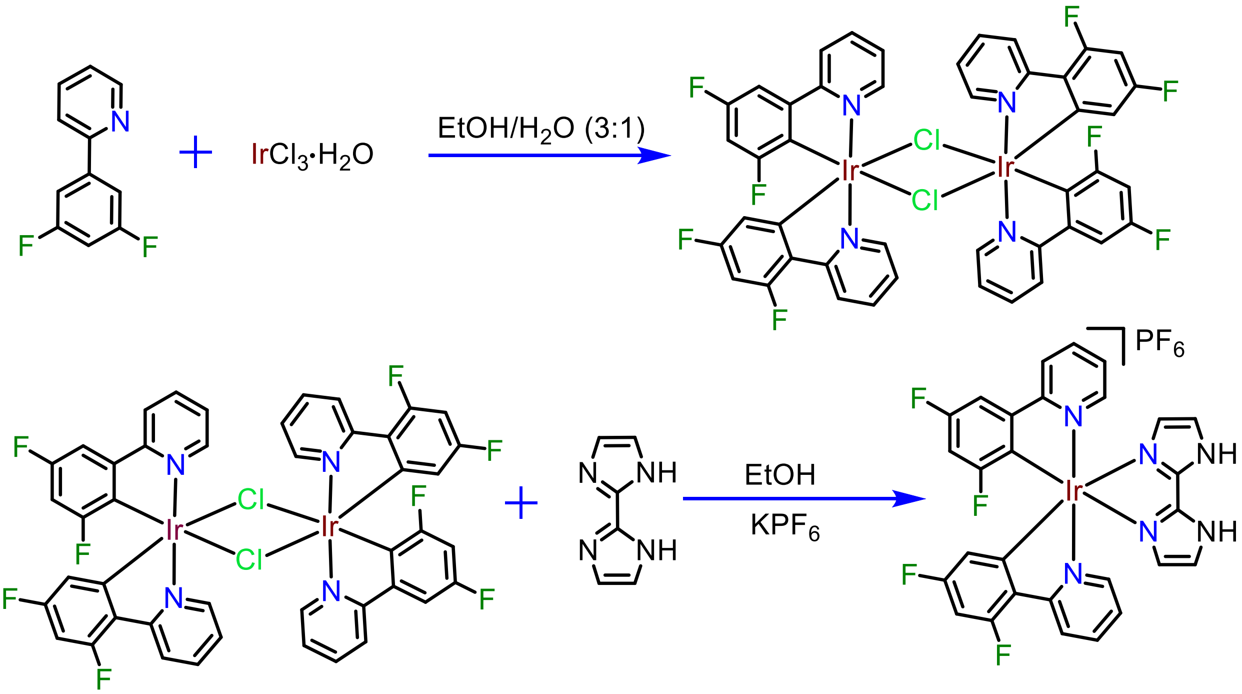

Scheme S5. Synthetic route for the formation of $[Ir^{III}(F_2ppy)_2(biimid)]PF_6$ complex

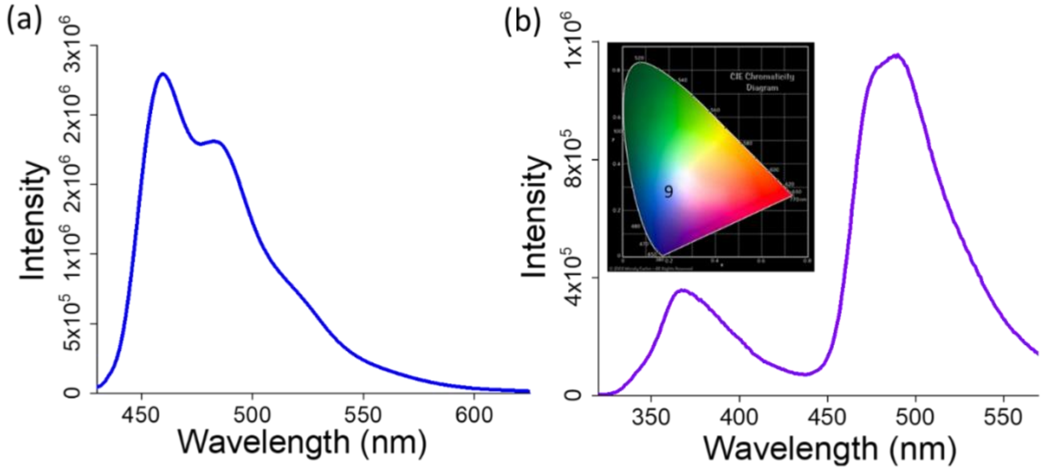

Fig. S8. Luminescence spectra of (a) $[Ir^{III}(F_2ppy)_2(biimid)]PF_6$ complex in MeCN (1.0×10^{-5} M) (λ_{ex} = 385 nm) and (b) Ir-L-F gel (λ_{ex} = 285 nm). Inset: CIE chromaticity diagram of Ir-L-F gel

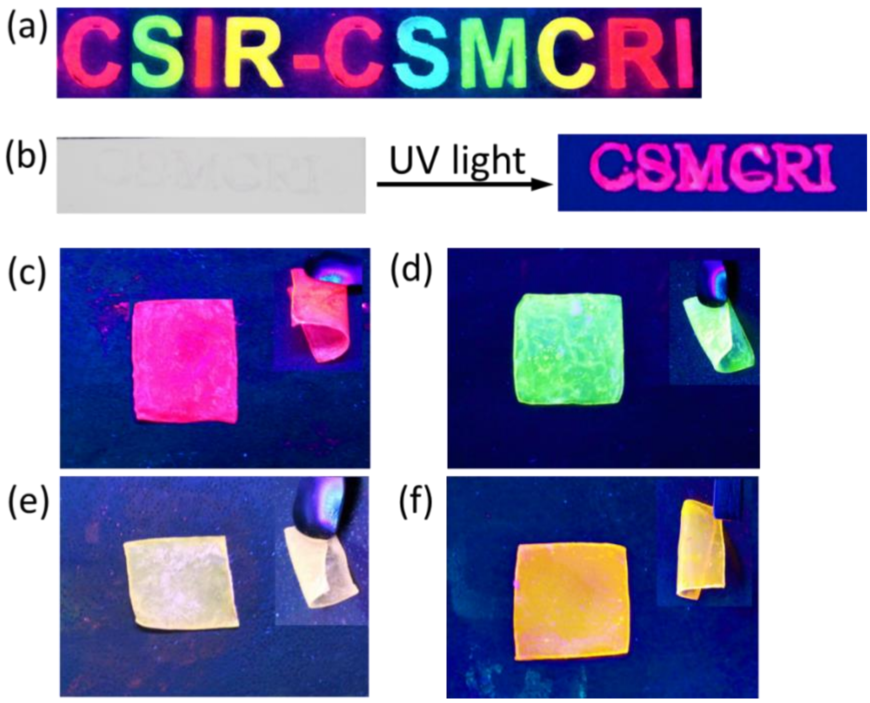

Fig. S9. (a) Photographs of write-up on a nonfluorescent glass plate using the metallogels under UV light irradiation (λ_{ex} = 365 nm), (b) Photographs of write-up on silica gel plate in daylight and after UV light irradiation, (c-f) The digital images of the (c) Eu•L-F, (d) Tb•L-F, (e) Eu•L-F-Tb•L-F, and (f) Eu•L-F-2(Tb•L-F) coated-agarose gel films. Inset: Corresponding luminescent films after bending

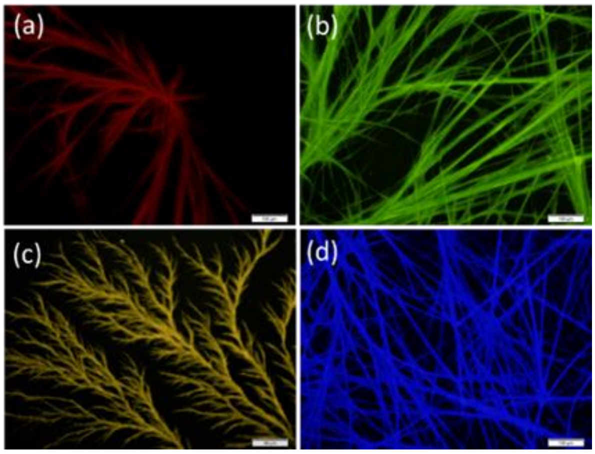

Fig. S10. Fluorescent microscope images of (a) Eu•L-F, (b) Tb•L-F, (c) Eu•L-F-2(Tb•L-F), and (d) Ir-L-F under fluorescence light

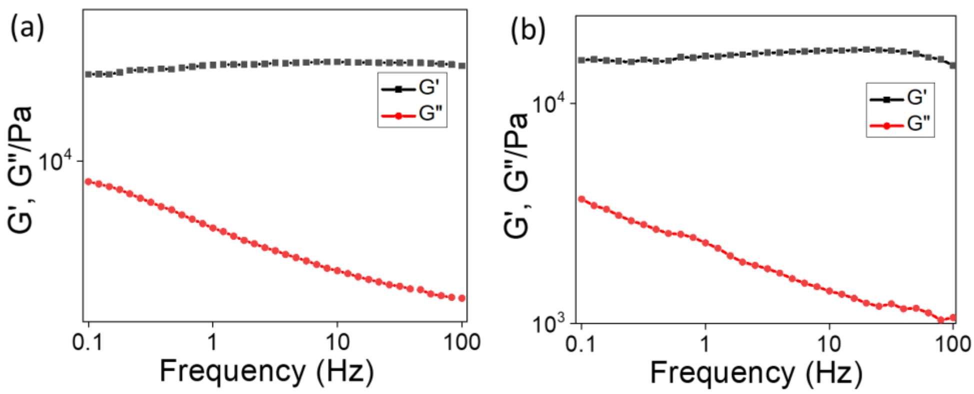

Fig. S11. Frequency sweeps at 0.1% strain amplitude of the storage modulus G′ (■) and loss modulus G″ (●) for (a) Eu•L-F and (b) Eu•L-F-Ir gels

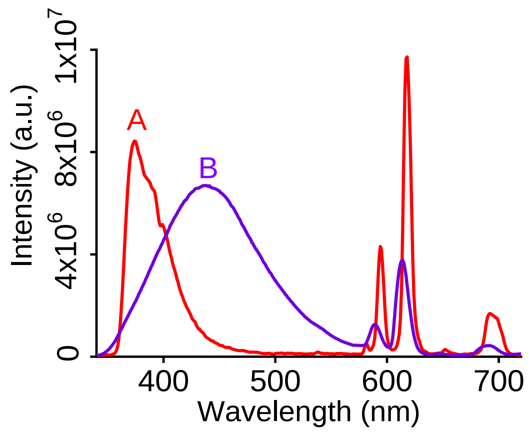

Fig. S12. Assessment of luminescence spectra of (A) Eu•L-F and (B) TFA exposed Eu•L-F sol generated after gel–sol transition